Biological Psychiatry: Celebrating 50 Years

Archival Report

Hyperperfusion of Frontal White and Subcortical Gray Matter in Autism Spectrum Disorder

Bradley S. Peterson, Ariana Zargarian, Jarod B. Peterson, Suzanne Goh, Siddhant Sawardekar, Steven C.R. Williams, David J. Lythgoe, Fernando O. Zelaya, and Ravi Bansal

ABSTRACT

BACKGROUND: Our aim was to assess resting cerebral blood flow (rCBF) in children and adults with autism spectrum disorder (ASD).

METHODS: We acquired pulsed arterial spin labeling magnetic resonance imaging data in 44 generally high-functioning participants with ASD simplex and 66 typically developing control subjects with comparable mean full-scale IQs. We compared rCBF values voxelwise across diagnostic groups and assessed correlations with symptom scores. We also assessed the moderating influences of participant age, sex, and IQ on our findings and the correlations of rCBF with *N*-acetylaspartate metabolite levels.

RESULTS: We detected significantly higher rCBF values throughout frontal white matter and subcortical gray matter in participants with ASD. rCBF correlated positively with socialization deficits in participants with ASD in regions where hyperperfusion was greatest. rCBF declined with increasing IQ in the typically developing group, a correlation that was absent in participants with ASD, whose rCBF values were elevated across all IQ levels. rCBF in the ASD group correlated inversely with *N*-acetylaspartate metabolite levels throughout the frontal white matter, with greater rCBF accompanying lower and increasingly abnormal *N*-acetylaspartate levels relative to those of typically developing control subjects.

CONCLUSIONS: These findings taken together suggest the presence of altered metabolism, likely of mitochondrial origin, and dysfunctional maintenance processes that support axonal functioning in ASD. These disturbances in turn likely reduce neural efficiency for cognitive and social functioning and trigger compensatory responses from supporting glial cells, which subsequently increase rCBF to affected white matter. These findings, if confirmed, suggest cellular and molecular targets for novel therapeutics that address axonal pathology and bolster glial compensatory responses in ASD.

Keywords: Arterial spin labeling, Autism, Cerebral blood flow, Glia, Magnetic resonance imaging, White matter

https://doi.org/10.1016/j.biopsych.2018.11.026

Regional cerebral blood flow (rCBF) is a surrogate measure of brain metabolism, because blood flow and metabolism are usually tightly coupled (1–5). Arterial spin labeling (ASL) provides absolute and reproducible measures of rCBF (6,7) by magnetically labeling water in arterial blood as a diffusible tracer, analogous to the use of ^{15}O water in positron emission tomography (PET) scanning (8). Unlike PET, ASL does not require the use of a radioactive tracer and therefore can be used in children, and it is a less costly and procedurally less complicated process. Moreover, because perfusion signals are obtained by pairwise subtraction of adjacently acquired tagged and control images, ASL is less prone to motion artifact, low-frequency physiological noise, and baseline drift than is more conventional blood oxygen level–dependent functional imaging (9). Finally, perfusion maps quantify rCBF at every voxel in the brain, whereas task-based blood oxygen level–dependent imaging quantifies neural activity only in locations that the task activates, and results are often confounded by systematic biases in task performance across participants (10).

We are aware of only one previous preliminary study employing ASL in persons with autism spectrum disorder (ASD) and typically developing (TD) control subjects; this previous study had a limited sample size, included only children, and reported abnormalities (increased rCBF) only in cortical gray matter of the ASD group (11). PET metabolism studies and single-photon emission computed tomography rCBF studies in ASD have had small numbers of participants, and some have either employed sedation or compared against atypically developing patient control subjects; most have interrogated only gray matter, and their findings have been rather inconsistent. Nevertheless, fluorodeoxyglucose (FDG) PET studies generally have reported reduced metabolism in cortical gray matter [anterior cingulate, parietal (12,13), and temporal (14–16) cortices] and increased metabolism in occipital (17,18) and other cortical (19) regions. One preliminary

 ISSN: 0006-3223

PET study reported hyperperfusion of basal ganglia and posterior cingulate cortex in ASD (20), whereas larger FDG fluorine 18 PET studies have found reduced basal ganglia and thalamus metabolism (21,22). One FDG PET study assessed white matter (WM) metabolism explicitly, reporting higher metabolic rates that were greatest in prefrontal regions and the internal capsule (IC) in 25 adults with ASD compared with 55 TD adults during a verbal learning task (23). Single-photon emission computed tomography blood flow studies have generally reported reduced rCBF in temporal (24–31), parietal (25,30,31), and frontal (26,27,29–33) cortices and basal ganglia (28,31,33). Prior resting-state functional magnetic resonance imaging (MRI) studies have generally reported long-range underconnectivity and local overconnectivity (34–45), suggesting the presence of axonal pathology in ASD.

We aimed to exploit some of the advantages of ASL to compare rCBF across a large sample of children and adults with ASD and age-, sex-, and IQ-matched TD control subjects. We also assessed the voxelwise associations of ASL-based measures of rCBF and brain metabolism with magnetic resonance spectroscopy–based measures of *N*-acetylaspartate (NAA) (46) to understand how rCBF associates with this index of mitochondrial functioning (47–49), cellular metabolism (50), and neuronal abundance and viability (48,49). Based on the prior metabolism and blood flow findings in ASD, we hypothesized a priori that we would detect reduced cortical and increased WM rCBF in ASD. We also assessed the moderating effects of age, sex, and IQ on rCBF values in an effort to use rCBF values to parse the phenotypic heterogeneity of ASD. Finally, we assessed the voxelwise correlation of rCBF with measures of NAA in participants with ASD.

METHODS AND MATERIALS

Sample Ascertainment and Characterization

This was a subset of 110 participants (44 individuals with ASD, 66 TD individuals) drawn from a larger MRI study of 200 persons with ASD (simplex cases) and TD control subjects (36,46); the ASL pulse sequence was not available for the earliest recruited participants in the larger study. Participants with ASD were recruited through the Developmental Neuropsychiatry Clinic at Columbia University and through community awareness events. Because screening of participants occurred prior to the publication of DSM-5 diagnostic criteria for ASD, screening was based on DSM-IV-TR (51) criteria for pervasive developmental disorder (PDD). Potential participants were required to have a previous clinical DSM-IV-TR diagnosis of PDD and a score >15 on either the Social Communication Questionnaire Lifetime Version (52) or Autism-Spectrum Quotient (53). Exclusion criteria specific to ASD were known medical conditions associated with ASD (e.g., fragile X syndrome, tuberous sclerosis). The final consensus diagnoses were established by a physician or clinical psychologist with established reliability by administering module 3 (n = 16) or module 4 (n = 25) of the Autism Diagnostic Observation Schedule–Generic (ADOS-G) (54). The revised algorithm was used for all modules (55,56). Diagnoses for younger participants were also aided by administering the Autism Diagnostic Interview–Revised to the participants' parents (57) (n = 17). In our final sample, 12 individuals (27%) met DSM-IV-TR criteria for autistic disorder, 23 (52%) for Asperger's disorder, and 8 (18%) for PDD–not otherwise specified. Because substantial evidence suggests that most individuals with DSM-IV–based PDD diagnoses also meet DSM-5 criteria for a diagnosis of ASD (58), for ease of reference we herein use the DSM-5 designation.

TD participants were recruited through flyers, online advertisements, and random sampling from a telemarketing list of local households eligible for participation, group-matched to participants with ASD on age, sex, and ethnicity. TD control subjects participated after a clinical interview including the Kiddie Schedule for Affective Disorders and Schizophrenia Present and Lifetime Version (59) for those younger than 18 years of age or the Structured Clinical Interview for DSM-IV Axis I Disorders (60) for those 18 years of age or older. Additional exclusion criteria for all participants included contraindications to MRI, a history of premature birth (<36 weeks), low birth weight (<2000 g), birth complications or injury, prior head trauma with loss of consciousness, seizures, or chronic medical illness. The Institutional Review Board of the New York State Psychiatric Institute approved the study procedures. An independent clinical monitor assessed the capacity for all adult participants with ASD to provide informed consent. One participant was deemed to lack that capacity and therefore designated a surrogate to provide it. All children provided written assent.

IQ for 1 participant with ASD was assessed using the Wechsler Intelligence Scale for Children (61) and for another using the Wechsler Adult Intelligence Scale (62); all other participants in the ASD and TD groups were assessed using the Wechsler Abbreviated Scale of Intelligence (63). As all participants with ASD had fluent speech, full-scale IQ (FSIQ) was available for all but one. The Edinburgh Handedness Inventory assessed laterality of handedness (64), and the Hollingshead Four-Factor Index estimated socioeconomic status (65).

MRI Scanning and Processing

All participants were unsedated for the scan. Details for scanning procedures, MRI pulse sequences, scan times, and image processing methods are provided in the Supplement.

Statistical Analyses

All group-level statistical analyses employed a general linear model at each voxel of the spatially normalized, individual rCBF maps, while covarying for age and sex, applying a false discovery rate procedure at 0.05 to control for false-positives and color-coding voxels on the T1 template where p values survived the false discovery rate procedure. All statistical models were hierarchically well formulated, with any interaction terms including the component main effects. Our a priori hypothesis assessed the main effect of diagnosis on rCBF in all participants with no other covariates or interactions in the model. We also assessed the influences of FSIQ and medication use on our findings in post hoc analyses by covarying separately for FSIQ and psychotropic medication use and by applying again our model for a priori hypothesis testing while excluding any participants with

ASD who were taking psychotropic medications at the time of scan.

Secondary analyses assessed the moderating effects of age, sex, and FSIQ on group differences in separate models that included the respective interactions with their component main effects. These interactions assessed whether the slopes of the correlations differed across the ASD and TD control groups. In addition, within the ASD group we assessed the correlations of rCBF with total and domain scores on the developmentally appropriate ADOS-G module and with standardized total and subscale scores on the Social Responsiveness Scale (SRS), while covarying for age and sex. We also assessed the voxelwise correlations of rCBF with magnetic resonance spectroscopy–based measures of NAA metabolite levels as a continuous variable, and we compared rCBF values in the 6 participants with ASD in whom we previously detected the presence of lactate with those of 30 participants with ASD in whom we did not detect the presence of lactate.

RESULTS

Sample Characteristics

The ASD and TD samples did not differ significantly in age, sex, ethnicity, FSIQ, handedness, or socioeconomic status (Table 1). By design, all SRS subscale scores were higher in the ASD sample (all $p < 10^{-11}$), reflecting more severe social symptoms (Table 1). Of the 44 participants with ASD, 14 (and no TD participants) were taking psychotropic medication at the time of scan: stimulants (n = 5), antidepressants (n = 7; includes selective serotonin reuptake inhibitors and serotonin and norepinephrine reuptake inhibitors), lithium (n = 2), anticonvulsants and/or mood stabilizers (n = 1), antipsychotics (n = 4), benzodiazepine (n = 2), monoamine oxidase inhibitor (n = 1), and nonstimulant attention-deficit/hyperactivity disorder medication (n = 2) (these total >14 because some individuals were taking multiple medications).

Group Comparisons of rCBF

Participants with ASD compared with TD participants had higher rCBF values throughout large expanses of WM, primarily in frontal regions comprising the centrum semiovale (CS), corona radiata, and IC bilaterally. They also had greater rCBF bilaterally in the gray matter of the caudate and lenticular nucleus more dorsally, the ventral striatum (VS), orbitofrontal cortex, and amygdala (Figure 1).

Correlations of rCBF With ASD Symptom Scores

Within the ASD group, rCBF correlated positively with the ADOS-G total score in many of the same frontal WM regions where a main effect of diagnosis was located (CS, corona

Table 1. Participant Characteristics

	ASD Group	TD Group	Test Statistic	*df*	*p* Value
n	44	66			
Mean Age, Years, Mean ± SD	24.9 ± 15.6	22.0 ± 11.2	t = 1.1	108	.26
Age Range, Years	5.9–60.7	6.9–59.0			
Sex, Male/Female, *n*	32/12	50/16	χ^2 = 0.13	1	.72
SES, Mean ± SD[a]	48.8 ± 10.5	53.5 ± 11.1	t = 1.90	85	.06
Handedness, Right/Left, *n*	38/6	62/4	χ^2 = 2.8	1	.11
Ethnic/Racial Minority, *n*	9	18	χ^2 = 0.77	1	.38
Framewise Motion, mm, Mean ± SD	0.17 ± 0.06	0.16 ± 0.06	t = 0.88	109	.37
RMS Motion, mm, Mean ± SD	0.09 ± 0.03	0.09 ± 0.04	t = 0.89	109	.37
FSIQ, Mean ± SD[b]	112.3 ± 18.3	116.7 ± 10.6	t = 1.42	60.8	.16
ADOS Score, Mean ± SD[c]					
Total	10.8 ± 4.1	—			
Social Affect	9.1 ± 3.8	—			
Restrict and Repet Beh	1.7 ± 1.6	—			
SRS Score, Mean ± SD[d]					
Total	83.0 ± 27.2	20.8 ± 18.3	t = 12.1	61.8	4×10^{-14}
Awareness	10.6 ± 3.3	5.1 ± 3.2	t = 7.8	85	1×10^{-11}
Cognition	15.4 ± 4.8	3.1 ± 3.6	t = 13.3	66.7	2×10^{-20}
Communication	28.4 ± 9.0	6.2 ± 7.2	t = 12.8	85	1×10^{-21}
Motivation	13.7 ± 5.3	3.5 ± 3.3	t = 10.4	58.8	7×10^{-15}
Mannerisms	15.6 ± 6.9	3.0 ± 3.8	t = 10.1	53.9	4×10^{-14}

ADOS, Autism Diagnostic Observation Schedule; ASD, autism spectrum disorder; Awareness, Social Awareness subscale; Cognition, Social Cognition subscale; Communication, Social Communication subscale; FSIQ, full-scale IQ; Motivation, Social Motivation subscale; Mannerisms, Restricted Interests and Repetitive Behaviors subscale; Restrict and Repet Beh, Restricted and Repetitive Behaviors domain; RMS Motion, root mean square motion estimate during the arterial spin labeling scan; SES, socioeconomic status; SRS, Social Responsiveness Scale; TD, typically developing.

[a]SES, measured with the Hollingshead, was available for 31 participants in the ASD group and 56 participants in the TD group.

[b]FSIQ was available for 43 participants in the ASD group and 65 participants in the TD group.

[c]ADOS scores were available for 41 participants in the ASD group.

[d]SRS scores were available for 38 participants in the ASD group and 49 participants in the TD group.

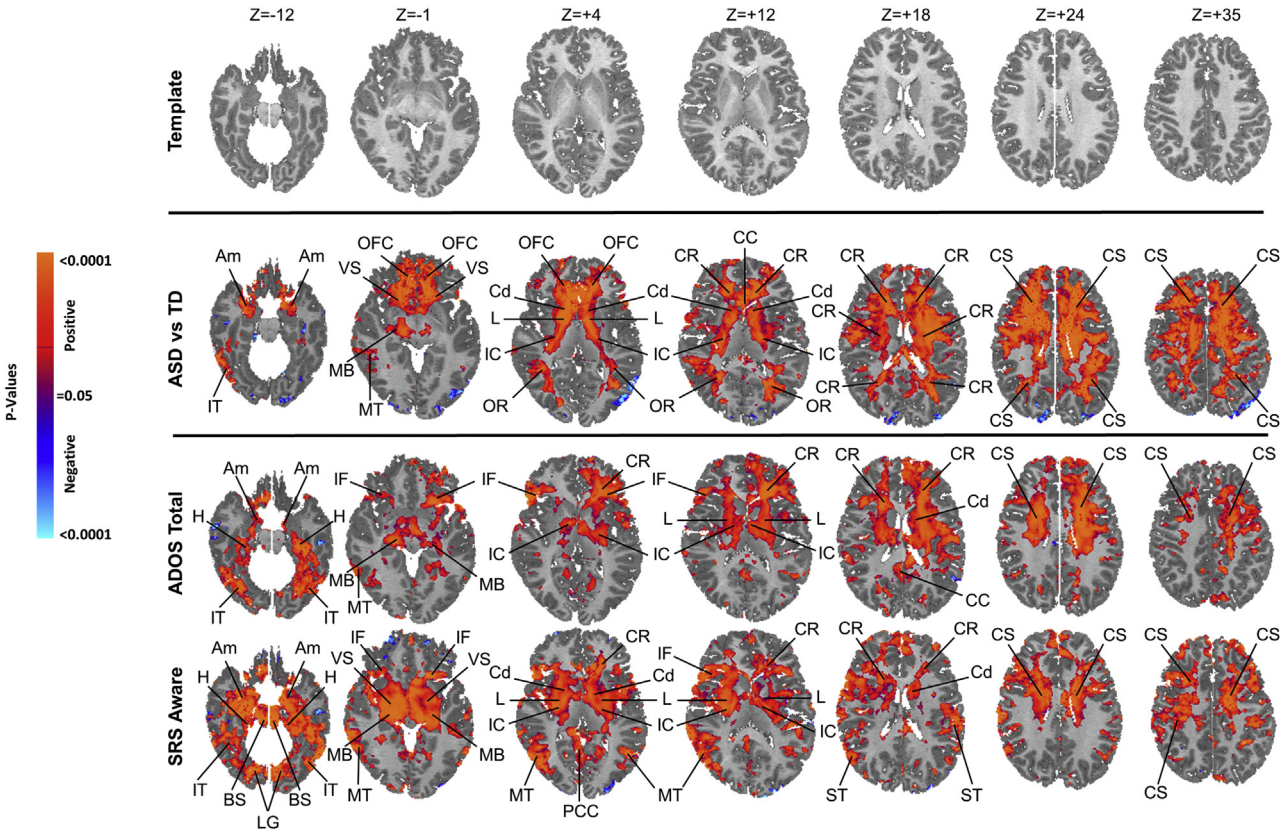

Figure 1. Group comparisons and symptom correlations. The right sides of the images correspond to the right side of the brain. All analyses control for the effects of age and sex, and the significance levels in all maps are false discovery rate–corrected for the number of statistical comparisons. (Top panel) The images show the T1-weighted anatomical template to which resting cerebral blood flow (rCBF) values for all participants were mapped at transaxial slice levels positioned parallel to the anterior commissure–posterior commissure line and corresponding to the positioning of the statistical maps shown in the other rows. The Z values represent slice level (in millimeters) in the Talairach coordinate system. (Middle panel) This shows the statistically significant differences in rCBF values between the autism spectrum disorder (ASD) group and typically developing (TD) control subjects while covarying for age and sex, displayed at a threshold of $p < .05$ after correction for multiple comparisons. Voxels in red indicate significantly increased rCBF, and blue voxels reduced rCBF, in ASD-group subjects relative to that in control subjects. Perfusion values at rest in the ASD group were higher bilaterally throughout white matter of all the frontal lobe, internal capsule (IC), and dorsal parietal lobe, and in gray matter of the basal ganglia, thalamus (Th), and amygdala (Am). (Bottom panel) Red and blue voxels represent, respectively, significant positive or inverse correlations of Autism Diagnostic Observation Schedule (ADOS) total scores and Social Responsiveness Scale (SRS) Social Awareness scores with rCBF values in the ASD group, after false discovery rate correction for multiple comparisons. BS, brain stem; CC, corpus callosum; Cd, caudate; CR, corona radiata; CS, centrum semovale; H, hippocampus; IF, inferior frontal gyrus; IT, inferior temporal gyrus; L, lenticular nucleus; LG, lingual gyrus; MB, midbrain; MT, middle temporal gyrus; OFC, orbitofrontal cortex; OR, optic radiations; PCC, posterior cingulate cortex; ST, superior temporal gyrus; VS, ventral striatum.

radiata), as well as within the hypothalamus, hippocampus, and middle temporal gyrus (Figure 1). The Social Affect domain score of the ADOS-G almost exclusively contributed to this correlation, with little or no contribution from the Repetitive Behaviors domain score (Supplemental Figures S22 and S23). Of the various SRS subscale scores, Social Awareness correlated most robustly with rCBF measures, both within more dorsal WM of the frontal lobe (CS) and in the gray matter of the hypothalamus, hippocampus, middle temporal gyrus, basal ganglia (caudate, lenticular nucleus, and VS), amygdala, hippocampus, and brain stem (Supplemental Figures S24–S28).

Moderators of Diagnosis Effect

Age significantly moderated the effects of diagnosis in the subgenual, pregenual, and dorsal anterior cingulate cortex (ACC), inferior frontal gyrus, dorsolateral prefrontal cortex, occipital gyrus, middle and inferior temporal gyrus, and amygdala (Figure 2), with the effects deriving in each instance from a steeper inverse correlation of rCBF with age in the ASD group than in TD control subjects (Figure 3).

Sex significantly moderated the effect of diagnosis, though the moderation was localized almost exclusively to the subgenual and pregenual ACC and small portions of the caudate, VS, and amygdala (Figure 2), with the effects deriving in each case from a reversal in the ASD group of the female > male rCBF differences present in TD control subjects (Figure 3).

FSIQ also significantly moderated the effect of diagnosis within frontal WM (corona radiata, CS, IC), hypothalamus, and insular cortex (Figure 2), with the effect in each case deriving from a steeper decline in FSIQ with increasing rCBF, and more broadly throughout frontal WM and subcortical gray matter, in

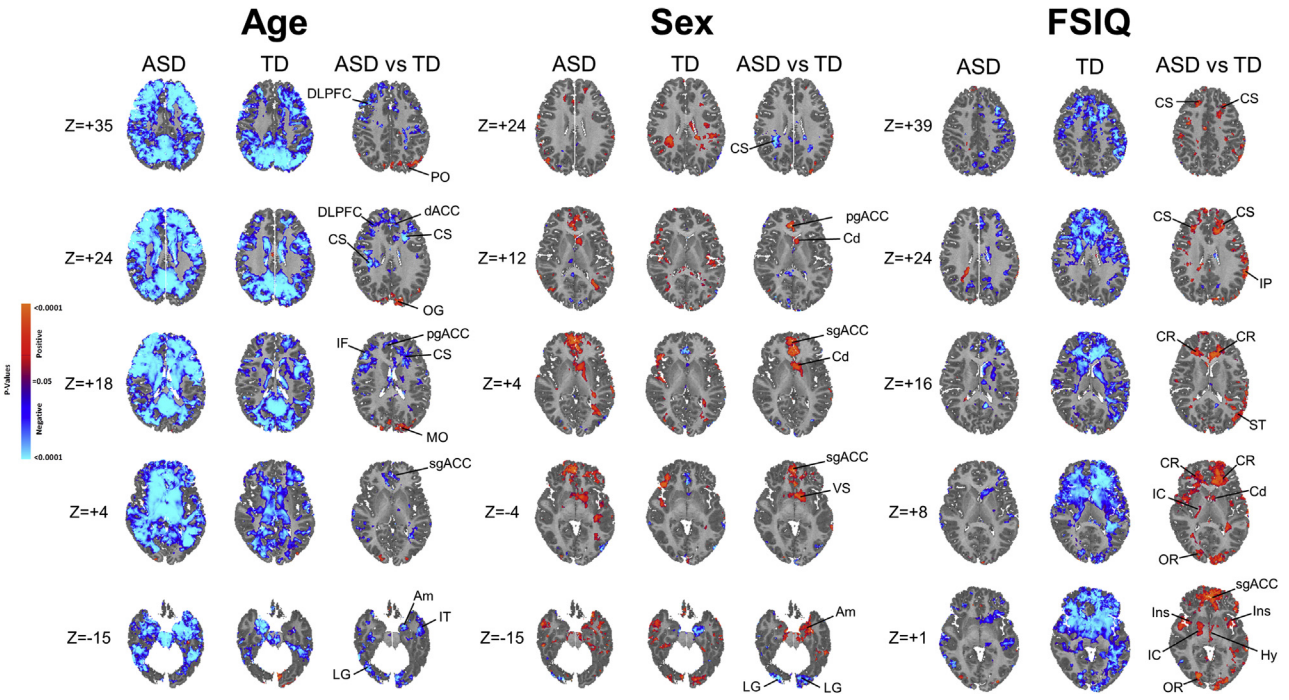

Figure 2. Maps showing the modifying effects of age, sex, and full-scale IQ (FSIQ). The significance levels in all maps are false discovery rate–corrected for the number of statistical comparisons. The Z values represent slice level (in millimeters) in the Talairach coordinate system. (Left panel) In the first two columns, maps show the significance of age correlations with resting cerebral blood flow (rCBF) at each voxel in the autism spectrum disorder (ASD) and typically developing (TD) groups separately, while covarying for sex. Red and blue voxels represent, respectively, significant positive or inverse correlations of age with rCBF values. The third column shows effects of the interaction of age with diagnosis on rCBF at each voxel, or the voxels where the correlations of age with rCBF differ significantly across the ASD and TD groups, while covarying for sex and including the main effects of age and diagnosis in a hierarchically well-formulated statistical model. (Middle panel) In the first two columns, maps show the significance of sex difference in rCBF at each voxel in the ASD and TD groups separately, while covarying for age. Red and blue voxels represent significantly higher rCBF values in male subjects or female subjects, respectively. The third column shows effects of the interaction of sex with diagnosis on rCBF at each voxel, or the voxels where sex differences in rCBF differ significantly across the ASD and TD groups, while covarying for age and including the main effects of sex and diagnosis in a hierarchically well formulated statistical model. (Right panel) In the first two columns, maps show the significance of correlations of FSIQ with resting rCBF at each voxel in the ASD and TD groups separately, while covarying for age and sex. Red and blue voxels represent, respectively, significant positive or inverse correlations of FSIQ with rCBF values. The third column shows effects of the interaction of FSIQ with diagnosis on rCBF at each voxel, or the voxels where the correlations of FSIQ with rCBF differ significantly across the ASD and TD groups, while covarying for age and sex and including the main effects of FSIQ and diagnosis in a hierarchically well formulated statistical model. Am, amygdala; Cd, caudate; CR, corona radiata; CS, centrum semiovale; dACC, dorsal anterior cingulate cortex; DLPFC, dorsolateral prefrontal cortex; Hy, hypothalamus; IC, internal capsule; IF, inferior frontal gyrus; Ins, insula; IP, inferior parietal; IT, inferior temporal gyrus; LG, lingual gyrus; MO, middle occipital gyrus; OG, occipital gyrus; OR, optic radiations; pgACC, pregenual anterior cingulate cortex; PO, parieto-occipital region; sgACC, subgenual anterior cingulate cortex; ST, superior temporal gyrus; VS, ventral striatum.

the TD control subjects than in the participants with ASD (Figure 3).

Correlations of rCBF With Magnetic Resonance Spectroscopy Metabolites

In the ASD and TD groups, separately and combined, rCBF correlated inversely with NAA metabolite levels throughout the frontal WM, as well as in the WM of the internal and external capsules (Figure 4). The 6 participants with ASD who had detectable lactate in their brains, compared with the 30 who did not, had significantly lower rCBF in the WM of the corpus callosum genu and posterior CS and in the gray matter of the dorsal prefrontal cortex and pregenual ACC. They also had higher rCBF values in the midcingulate cortex (Figure 4).

Post Hoc Analyses

We conducted post hoc analyses to assess the effects of potential confounds on our findings. Covarying for FSIQ in our models had negligible effects on our findings (Supplemental Figures S29–S31). Likewise, covarying for the use of psychotropic medications at the time of MRI scan had negligible effects, as did excluding from analyses those participants with ASD taking psychotropic medications, though maps were overall somewhat less statistically significant because of reduced statistical power associated with fewer participants (Supplemental Figures S32–S37). Covarying for total cortical gray matter or total WM volumes also had no discernible effects on our findings (Supplemental Figures S38–S39). Finally, we also conducted our primary analyses (shown in Figure 1) separately in youths (≤21 years of age; n = 20) and adults (>21 years of age; n = 24); despite the reduced statistical power, hyperperfusion was found in both groups, with the most prominent hyperperfusion in frontal locations in the youth group and in the dorsal parietal location in the adult group (Supplemental Figure S40). rCBF correlations with ADOS-G total scores were stronger in adults with ASD, whereas SRS

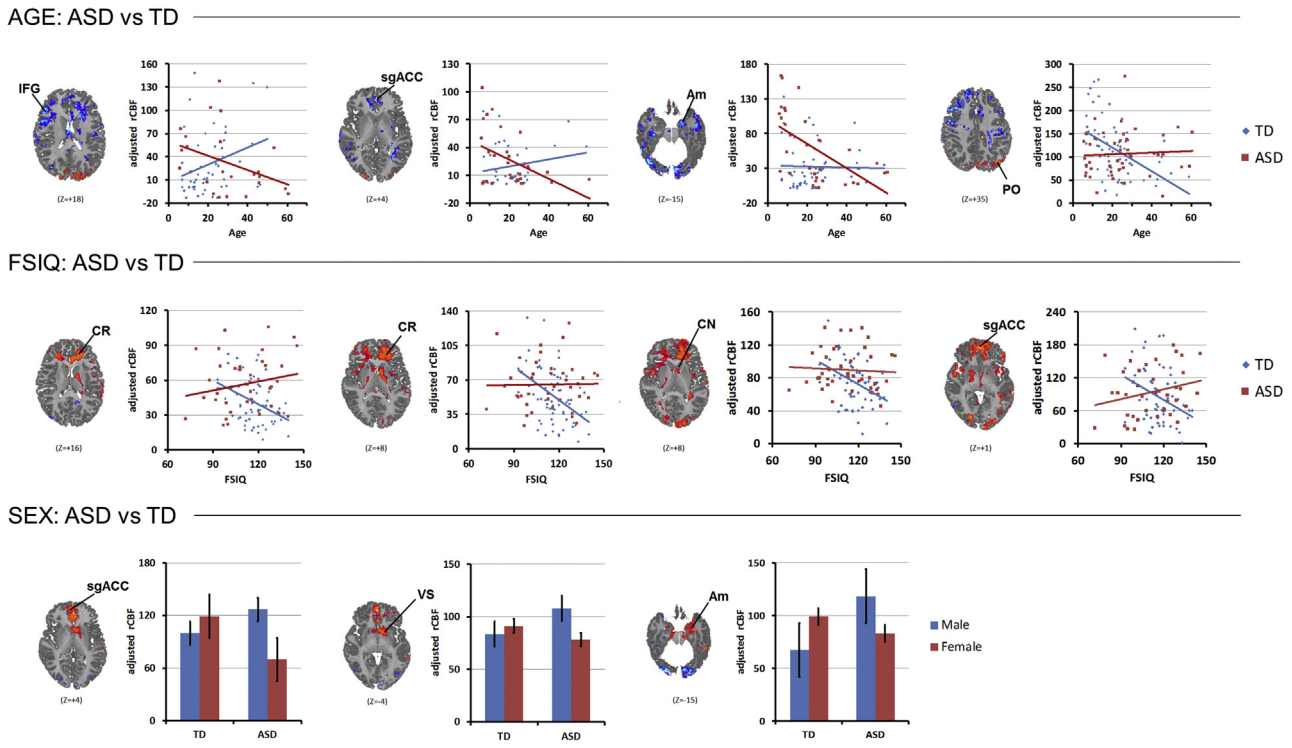

Figure 3. Data displays for age, sex, and full-scale IQ (FSIQ) effects. These are shown for representative regions indicated from a slice taken from Figure 2, shown above each plot in the statistical map. The Z values represent slice level (in millimeters) in the Talairach coordinate system. The line leading from the regional label to the image indicates the voxels with the images that were sampled to generate the data shown in the scatter plots. The scatter plots illustrate the age-related decline in resting cerebral blood flow (rCBF) in most cortical regions for autism spectrum disorder (ASD) and the inverse correlation of rCBF with FSIQ in the typically developing (TD) but not in the ASD group. Bar graphs for sex effects show in ASD participants the reversal of female > male rCBF sex differences present in the TD group. Error bars represent standard error. Participant age is given in years. Am, amygdala; CN, caudate nucleus; CR, corona radiata; IFG, inferior frontal gyrus; PO, parieto-occipital region; sgACC, subgenual anterior cingulate cortex; VS, ventral striatum.

Awareness correlations were stronger in youths with ASD (Supplemental Figures S41 and S42).

DISCUSSION

To the best of our knowledge, this is the first report of widespread hyperperfusion in ASD, and the first to report voxelwise correlations of rCBF with NAA metabolite concentrations throughout the brain.

Hyperperfusion in ASD

Hyperperfusion was present throughout the frontal WM and subcortical gray matter in participants with ASD of all ages and of both sexes. Within the ASD group, rCBF correlated positively with measures of socialization deficits, including Social Affect domain scores on the ADOS-G and the Social Awareness subscale of the SRS, in regions where hyperperfusion in group comparisons of rCBF were greatest.

Our findings of WM hyperperfusion are consistent with the results of one prior study of FDG PET brain metabolism, which reported higher metabolic rates in the WM of 25 adults with ASD compared with 55 TD adults performing a verbal learning task, with the greatest increases in the prefrontal WM and the anterior limb of the IC (23). They are also consistent with findings from numerous MRI (66,67) and diffusion tensor imaging (68,69) studies reporting volumetric and organizational WM abnormalities in persons with ASD, and with postmortem findings of fewer long axons, more short local axons, and thinner myelin (70,71), which together suggest that compromised integrity of axons or oligodendrocytes may be the anatomical basis for reported long-range underconnectivity and local overconnectivity in functional MRI studies (34–45).

Central nervous system WM consumes approximately one third the energy that gray matter does (1–5) because of the greater energy efficiency of axon action potentials and especially WM synapses (73). Most WM energy is devoted to maintaining resting potentials and various housekeeping tasks (72,73). Hyperperfusion in ASD could derive from pathology in any one or a combination of these maintenance processes in neuronal axons, the most abundant cellular tissue in WM and its largest component by volume.

Oligodendrocytes, which comprise approximately 5% of all cells and 10% to 15% of all human glial cells in the brain (74,75), ensheath WM axons with myelin to speed saltatory conduction (76). Their pathological functioning could alter myelination and, secondarily, WM metabolism and perfusion. Myelination is particularly important for finely calibrating conduction speeds and coordinating signals over long axons, which functional MRI studies have suggested is a prominent disturbance in ASD (34–45). Most new myelin in

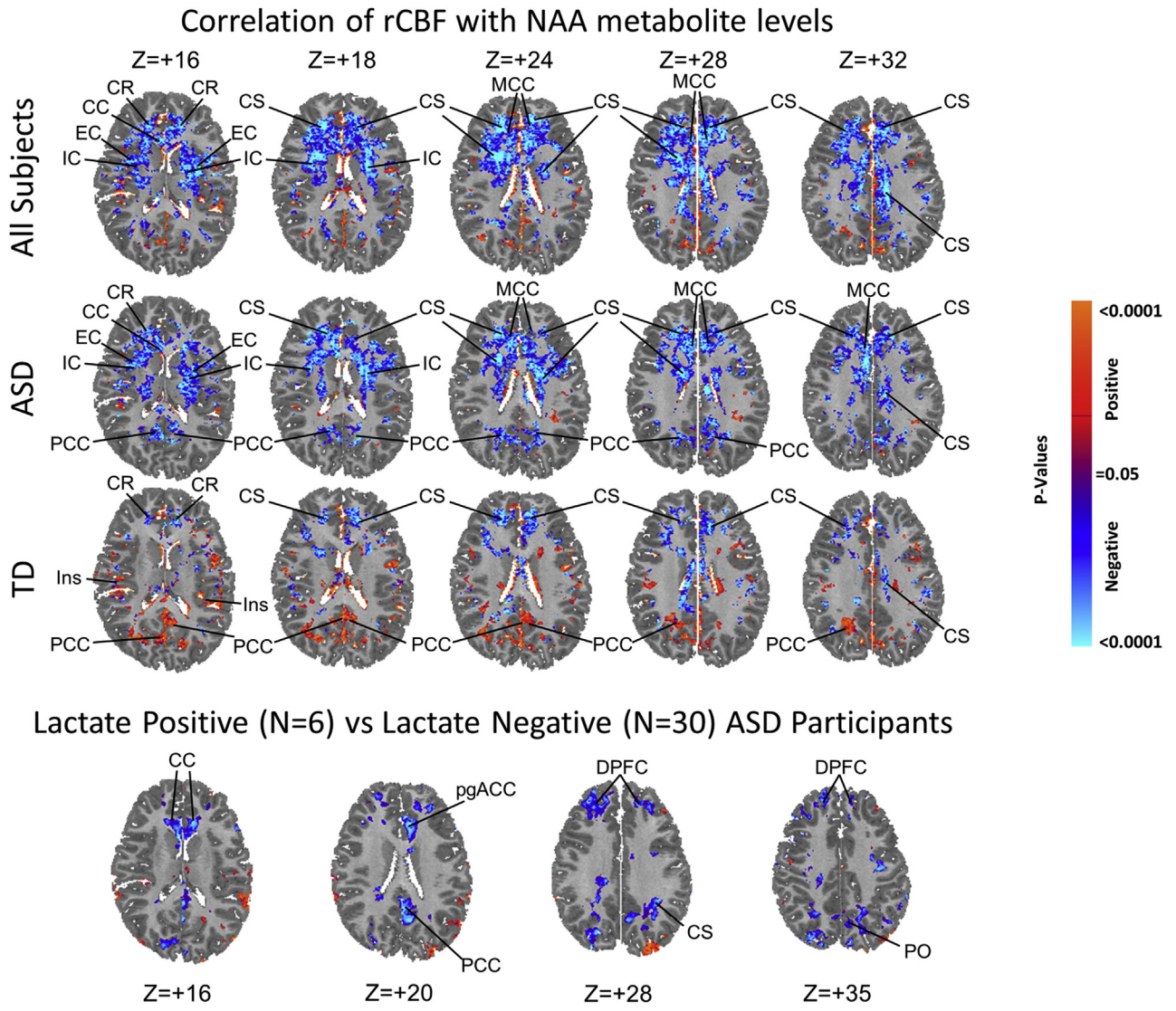

Figure 4. Correlations of resting cerebral blood flow (rCBF) with *N*-acetylaspartate (NAA) metabolite levels and lactate. The three rows in the top panel show the voxelwise correlations of NAA level with rCBF in the autism spectrum disorder (ASD) (n = 36, 29 male subjects, 7 female subjects; mean age 25.6 years) and typically developing (TD) (n = 63, 48 male subjects, 15 female subjects; mean age 22.3 years) groups combined (top row) and separately (bottom two rows), while covarying for age and sex. Significance levels are false discovery rate–corrected for the number of statistical comparisons. The Z values represent slice level (in millimeters) in the Talairach coordinate system. Primarily inverse correlations (blue voxels) are present in the ASD group in the frontal white matter of the centrum semiovale (CS) and corona radiata (CR), internal capsule (IC), and external capsule (EC), and in the midcingulate cortex (MCC) and posterior cingulate cortex (PCC). In the TD group, inverse correlations are seen in similar locations, but they are smaller in spatial extent and weaker in statistical significance; positive correlations (red voxels) in the TD group are scattered throughout cortical gray matter (insula [Ins], posterior cingulate cortex [PCC]), and inverse correlations are present in frontal white matter (CS, CR). (Bottom panel) The 6 ASD participants with detectable lactate compared with the 30 without detectable lactate had significantly lower rCBF values (blue voxels) in the dorsal prefrontal cortex (DPFC), pregenual anterior cingulate cortex (pgACC), PCC, genu of the corpus callosum (CC), and posterior white matter of the CS and parieto-occipital region (PO).

adulthood is formed through an activity-dependent, plastic remodeling of the number, length, and thickness of preexisting myelin sheaths (37,77–84). Approximately 20% of new myelin in adulthood also derives from the neuronal activity–dependent differentiation of oligodendrocyte precursor cells into new oligodendrocytes (84–86). Thus, primary abnormalities in oligodendrocytes could produce altered WM metabolism and blood flow; alternatively, abnormalities in axonal activity, whether from molecular or genetic defects in ASD or from altered experiences associated with the disorder, could in turn trigger ongoing, activity-dependent myelin remodeling and its attendant increased metabolic demands.

Astrocytes, the most abundant glial cell type in the central nervous system, constitute nearly half the volume of the WM and contribute significantly to WM metabolism and blood flow (87). They play an essential supporting role in oligodendrocyte precursor cell proliferation and differentiation,

production of myelin (88), and formation of the blood-brain barrier. They take up potassium and glutamate released into the interstitial fluid to sustain and modulate high-frequency neuronal firing. Though they are not electrically excitable, their gap junctions form a large network of astrocyte signaling that propagates calcium ion and adenosine triphosphate (ATP) waves over long distances (89,90). These properties of astrocytes are increasingly believed to play an important role in learning, memory, and intelligence (91), and genetic mutations affecting astrocyte functioning even produce ASD-like phenotypes of maturational delay, intellectual disability, and seizures (88). Altered astrocyte metabolism could account for our perfusion findings.

Microglia, the least abundant glial cell type, are the primary responders in a central nervous system cellular immune response. Their relative scarcity makes their metabolism itself an unlikely cause of hyperperfusion in ASD, though the inflammatory responses that they generate could increase perfusion. Excessive microglial cell number and activation have been reported in previous PET and postmortem studies of ASD (92–94). The reactive oxygen species and proinflammatory cytokines that excessive microglial cells generate could produce the impaired mitochondrial functioning suggested in previous studies (95), including one study of our participants (46).

Hyperperfusion was also present in the basal ganglia and amygdala. Though they are predominantly gray matter structures, they do contain axons, myelin, and glia (96,97), and therefore a disturbance affecting any one of these cell components could produce hyperperfusion in both WM and gray matter.

Interactions With Age

We detected a significantly steeper inverse correlation of rCBF with age in the ASD group than in TD control subjects throughout much of cortical gray matter, but most significantly in the ACC, dorsolateral prefrontal cortex, amygdala, and several other cortical gray matter regions, with rCBF generally higher in children and either similar or lower in adults with ASD compared with control subjects (Figure 2B). Thus, the hyperperfusion detected in ASD across all ages in WM and subcortical gray matter was also present in cortical gray matter and amygdala, but primarily in children with ASD. Prior ^{15}O water PET studies have reported declining cerebral metabolic rates (1–5) and blood flow (1–3,5) with age in cortical gray matter in healthy individuals; age correlates generally have not been reported in ASD. We detected an age-related decline of rCBF in healthy individuals only in the occipital cortex. A decline in rCBF in other cortical regions was found in participants with ASD, and in the direction toward values in healthy control subjects with advancing age, suggesting either that rCBF normalizes with age in cortical gray matter or that values close to normal in those regions may be a marker for ASD symptoms that persist into adulthood. By extension, higher rCBF values in children could also represent some kind of adaptive response to the presence of illness. Myriad cellular aging processes could account for the age-related decline in cortical rCBF in ASD, including fewer neurons (98), dendritic arbors, or spines; reduced activity of the synaptic sodium–potassium pump and resting membrane potential (99); or less oxygen consumption and energy production from neuronal mitochondria in older compared with younger participants with ASD (100).

Interactions With Sex

We detected a significant sex-by-diagnosis interaction effect on rCBF in limbic regions, including the subgenual ACC, VS, and amygdala, as well as in parietal WM (Figure 2). In each instance, rCBF was greater in TD female subjects than TD male subjects, but this sex difference reversed in the ASD group, driven by particularly high values in male subjects with ASD, higher than values in either TD male subjects or TD female subjects (Figure 2B). These findings suggest that for reasons unknown, the perfusion abnormalities and cellular processes underlying them in ASD are disproportionately greater in male subjects in limbic gray matter regions, perhaps contributing to the well-known male predominance in prevalence of ASD and to the more severe problems with externalizing and prosocial behaviors commonly found in male subjects with ASD (101,102).

Interactions With IQ

We detected a significant IQ-by-diagnosis interaction effect on rCBF values in the frontal WM and subcortical gray matter that derived from a significant decline in rCBF with increasing IQ in the TD group, a correlation that was absent in participants with ASD (Figure 2A, B). The hyperperfusion present in most members of the ASD group, though attenuated in younger participants with ASD, destroyed the normal association of IQ with rCBF in these regions (Figure 3). The inverse correlation of resting rCBF with IQ in the TD control subjects is consistent with the neural efficiency hypothesis of intelligence, which posits that those with higher intelligence process information more efficiently, using less energy to accomplish any given task (103). Presumably, this greater efficiency is present even in the resting brain that is not explicitly engaged in performing any task. The cellular and molecular determinants of greater efficiency are unknown, but they could include improved synaptic or network connectivity (104), myelination (104), or maintenance of resting potentials and other housekeeping functions (105,106). These need not be the same determinants as those that increase perfusion in ASD, but if they are the same, then disturbances in myelin remodeling or axon housekeeping functions are potential culprits in ASD, as both would require increased metabolism to support intellectual functioning at its highest potential.

Metabolite Correlations

rCBF throughout the frontal WM in the ASD group correlated inversely with NAA metabolite levels. We reported elsewhere significantly lower NAA concentrations in the ASD group compared with those in control subjects (B. Peterson *et al.*, M.D., unpublished data, July 2018). Thus, greater rCBF accompanied lower, and increasingly abnormal, NAA levels. As findings from prior studies indicate that reduced NAA concentrations represent a reduced density or functioning of axonal mitochondria (48,49), reduced frontal WM mitochondria could suggest that increased frontal WM rCBF and metabolism

represents a compensatory process in ensheathing glia to maintain the energy state of WM axons.

The possibility of compensation is bolstered by evidence that glia support the formidable metabolic housekeeping demands of myelinated axons, which are challenged by sparse mitochondria and slow passive diffusion of nutrients across nodes of Ranvier (107). Myelinating oligodendrocytes couple with associated axons to support neuronal metabolism under stress (108), in part through the release of exosomes containing trophic substances (72,73,108,109) and in part through the shuttling of lactate and pyruvate to axons to serve as substrates for aerobic ATP production (110). Axonal firing stimulates further oligodendrocyte production of lactate and pyruvate through the release of glutamate, which activates oligodendrocyte *N*-methyl-D-aspartate receptors to stimulate uptake of glucose and glycolysis, thereby maintaining energy supplies to axons (88,111,112). Finally, the myelin sheath has been proposed as an ectopic site of glucose combustion and ATP generation for use by myelinated axons (73,113–115), though direct experimental and mathematical-modeling support for ATP generation in myelin sheaths is lacking (116).

The positive correlations of rCBF with measures of social impairment we observed suggest that this putative compensatory response is either unsuccessful or incomplete, because fully successful compensation would produce an inverse correlation of rCBF with social impairment. In the presence of unsuccessful or incomplete compensation, however, greater reductions of NAA and axonal metabolism would produce more severe symptoms and a proportionately greater compensatory response in glial cell metabolism—i.e., it would produce the observed positive associations of social impairment with rCBF. Alternatively, sustained increases in myelin synthesis by oligodendrocytes in the WM of persons with ASD could deplete the associated axons of NAA, because more myelin synthesis would require transportation of more NAA from neurons to oligodendrocytes for cleavage and use of its acetate moiety (117,118). Increased myelin synthesis therefore could account for both reduced NAA in axons and increased rCBF in metabolic support of myelin synthesis. Human postmortem and imaging studies, however, generally have not provided evidence for excessive, ongoing myelination in ASD.

Limitations

Though our sample comprised participants with ASD having a wide range of intellectual and social functioning, mean IQs were by design comparable with those of TD participants to limit the potential confounding effects of IQ differences on our findings. This sample selection, however, limits the generalizability of our findings to persons who are more severely affected with ASD, at least with respect to language and cognitive functioning. In addition, a larger sample size would improve statistical power and the stability of interaction effects. Longitudinal imaging studies are needed to support developmentally based interpretations of our findings (10).

Conclusions

Extensive resting frontal WM hyperperfusion in ASD suggests increased metabolic demands of either axons or glia or both. Positive correlations of rCBF with measures of social impairment in the same WM regions suggest that increased perfusion either partially generates those symptoms or is a proportionate response to their presence. The altered associations of rCBF with IQ moreover suggest impaired neural efficiency in the frontal WM. The combination of reduced NAA levels with proportionally greater rCBF values in frontal WM suggests that glial cells are attempting unsuccessfully or incompletely to compensate for reduced axonal metabolism in ASD. The most parsimonious explanation for all these findings is the presence of axonal pathology, including reduced NAA and altered mitochondrial metabolism, that disrupts one or more components of the housekeeping processes supporting axonal functioning, thereby reducing the efficiency of information processing. These disruptions trigger compensatory responses from supporting glial cells to support axon metabolism and proportionately increase rCBF to affected WM. The compensatory response is only partial, however, and in the ASD group disrupts the normal association of greater efficiency of neural processing with increasing IQ observed in the TD group. These findings, if confirmed, suggest cellular and molecular targets for studies of axonal pathology and development of novel therapeutics to bolster glial compensatory responses in ASD.

ACKNOWLEDGMENTS AND DISCLOSURES

The research was made possible by the provision of data by New York State Psychiatric Institute and Columbia University. We thank Dr. Molly Algermissen for her technical assistance. This study was supported by the National Institute of Mental Health (Grant Nos. R01 MH089582 [to BSP] and 2T32MH16434 [to BSP]) and funding from Children's Hospital Los Angeles and the University of Southern California.

The authors report no biomedical financial interests or potential conflicts of interest.

ARTICLE INFORMATION

From the Institute for the Developing Mind (BSP, JBP, SS, RB), Children's Hospital Los Angeles; Keck School of Medicine (BSP, AZ, RB), University of Southern California, Los Angeles; and Cortica Healthcare (SG), San Diego, California; and Department of Neuroimaging (SCRW, DJL, FOZ), Institute of Psychiatry, Psychology and Neuroscience, King's College London, London, United Kingdom.

Address correspondence to Bradley S. Peterson, M.D., Children's Hospital Los Angeles, 4650 Sunset Boulevard, MS 135, Los Angeles, CA 90027; E-mail: bpeterson@chla.usc.edu.

Received Sep 10, 2018; revised Nov 21, 2018; accepted Nov 27, 2018.

Supplementary material cited in this article is available online at https://doi.org/10.1016/j.biopsych.2018.11.026.

REFERENCES

1. Marchal G, Rioux P, Petit-Taboue MC, Sette G, Travere JM, Le Poec C, *et al.* (1992): Regional cerebral oxygen consumption, blood flow, and blood volume in healthy human aging. Arch Neurol 49:1013–1020.
2. Lenzi GL, Frackowiak RS, Jones T, Heather JD, Lammertsma AA, Rhodes CG, *et al.* (1981): CMRO2 and CBF by the oxygen-15 inhalation technique. Results in normal volunteers and cerebrovascular patients. Eur Neurol 20:285–290.
3. Pantano P, Baron JC, Lebrun-Grandie P, Duquesnoy N, Bousser MG, Comar D (1984): Regional cerebral blood flow and oxygen consumption in human aging. Stroke 15:635–641.
4. Yamaguchi T, Kanno I, Uemura K, Shishido F, Inugami A, Ogawa T, *et al.* (1986): Reduction in regional cerebral metabolic rate of oxygen during human aging. Stroke 17:1220–1228.

5. Leenders KL, Perani D, Lammertsma AA, Heather JD, Buckingham P, Healy MJ, *et al.* (1990): Cerebral blood flow, blood volume and oxygen utilization. Normal values and effect of age. Brain 113(Pt 1): 27–47.
6. Floyd TF, Ratcliffe SJ, Wang J, Resch B, Detre JA (2003): Precision of the CASL-perfusion MRI technique for the measurement of cerebral blood flow in whole brain and vascular territories. J Magn Reson Imaging 18:649–655.
7. Detre JA, Wang J (2002): Technical aspects and utility of fMRI using BOLD and ASL. Clin Neurophysiol 113:621–634.
8. Detre JA, Zhang W, Roberts DA, Silva AC, Williams DS, Grandis DJ, *et al.* (1994): Tissue specific perfusion imaging using arterial spin labeling. NMR Biomed 7:75–82.
9. Wong EC, Buxton RB, Frank LR (1999): Quantitative perfusion imaging using arterial spin labeling. Neuroimaging Clin N Am 9: 333–342.
10. Horga G, Kaur T, Peterson BS (2014): Annual research review: Current limitations and future directions in MRI studies of child- and adult-onset developmental psychopathologies. J Child Psychol Psychiatry 55:659–680.
11. Jann K, Hernandez LM, Beck-Pancer D, McCarron R, Smith RX, Dapretto M, *et al.* (2015): Altered resting perfusion and functional connectivity of default mode network in youth with autism spectrum disorder. Brain Behav 5:e00358.
12. Haznedar MM, Buchsbaum MS, Metzger M, Solimando A, Spiegel-Cohen J, Hollander E (1997): Anterior cingulate gyrus volume and glucose metabolism in autistic disorder. Am J Psychiatry 154:1047–1050.
13. Haznedar MM, Buchsbaum MS, Wei TC, Hof PR, Cartwright C, Bienstock CA, *et al.* (2000): Limbic circuitry in patients with autism spectrum disorders studied with positron emission tomography and magnetic resonance imaging. Am J Psychiatry 157:1994–2001.
14. Zilbovicius M, Boddaert N, Belin P, Poline JB, Remy P, Mangin JF, *et al.* (2000): Temporal lobe dysfunction in childhood autism: A PET study. Positron emission tomography. Am J Psychiatry 157: 1988–1993.
15. Boddaert N, Chabane N, Barthelemy C, Bourgeois M, Poline JB, Brunelle F, *et al.* (2002): Bitemporal lobe dysfunction in infantile autism: Positron emission tomography study [in French]. J Radiol 83:1829–1833.
16. Dilber C, Caliskan M, Sonmezoglu K, Nisli S, Mukaddes NM, Tatli B, *et al.* (2013): Positron emission tomography findings in children with infantile spasms and autism. J Clin Neurosci 20:373–376.
17. Zurcher NR, Bhanot A, McDougle CJ, Hooker JM (2015): A systematic review of molecular imaging (PET and SPECT) in autism spectrum disorder: Current state and future research opportunities. Neurosci Biobehav Rev 52:56–73.
18. Hazlett EA, Buchsbaum MS, Hsieh P, Haznedar MM, Platholi J, LiCalzi EM, *et al.* (2004): Regional glucose metabolism within cortical Brodmann areas in healthy individuals and autistic patients. Neuropsychobiology 49:115–125.
19. Rumsey JM, Duara R, Grady C, Rapoport JL, Margolin RA, Rapoport SI, *et al.* (1985): Brain metabolism in autism. Resting cerebral glucose utilization rates as measured with positron emission tomography. Arch Gen Psychiatry 42:448–455.
20. Pagani M, Manouilenko I, Stone-Elander S, Odh R, Salmaso D, Hatherly R, *et al.* (2012): Brief Report: Alterations in cerebral blood flow as assessed by PET/CT in adults with autism spectrum disorder with normal IQ. J Autism Dev Disord 42:313–318.
21. Haznedar MM, Buchsbaum MS, Hazlett EA, LiCalzi EM, Cartwright C, Hollander E (2006): Volumetric analysis and three-dimensional glucose metabolic mapping of the striatum and thalamus in patients with autism spectrum disorders. Am J Psychiatry 163: 1252–1263.
22. Siegel BV Jr, Asarnow R, Tanguay P, Call JD, Abel L, Ho A, *et al.* (1992): Regional cerebral glucose metabolism and attention in adults with a history of childhood autism. J Neuropsychiatry Clin Neurosci 4:406–414.
23. Mitelman SA, Buchsbaum MS, Young DS, Haznedar MM, Hollander E, Shihabuddin L, *et al.* (2017): Increased white matter metabolic rates in autism spectrum disorder and schizophrenia. Brain Imaging Behav 12:1290–1305.
24. Carina Gillberg I, Bjure J, Uvebrant P, Vestergren E, Gillberg C (1993): SPECT (Single Photon Emission Computed Tomography) in 31 children and adolescents with autism and autistic-like conditions. Eur Child Adolesc Psychiatry 2:50–59.
25. Mountz JM, Tolbert LC, Lill DW, Katholi CR, Liu HG (1995): Functional deficits in autistic disorder: Characterization by technetium-99m-HMPAO and SPECT. J Nucl Med 36:1156–1162.
26. Hashimoto T, Sasaki M, Fukumizu M, Hanaoka S, Sugai K, Matsuda H (2000): Single-photon emission computed tomography of the brain in autism: Effect of the developmental level. Pediatr Neurol 23:416–420.
27. Ohnishi T, Matsuda H, Hashimoto T, Kunihiro T, Nishikawa M, Uema T, *et al.* (2000): Abnormal regional cerebral blood flow in childhood autism. Brain 123(Pt 9):1838–1844.
28. Starkstein SE, Vazquez S, Vrancic D, Nanclares V, Manes F, Piven J, *et al.* (2000): SPECT findings in mentally retarded autistic individuals. J Neuropsychiatry Clin Neurosci 12:370–375.
29. Kaya M, Karasalihoglu S, Ustun F, Gultekin A, Cermik TF, Fazlioglu Y, *et al.* (2002): The relationship between 99mTc-HMPAO brain SPECT and the scores of real life rating scale in autistic children. Brain Dev 24:77–81.
30. Burroni L, Orsi A, Monti L, Hayek Y, Rocchi R, Vattimo AG (2008): Regional cerebral blood flow in childhood autism: A SPET study with SPM evaluation. Nucl Med Commun 29:150–156.
31. Degirmenci B, Miral S, Kaya GC, Iyilikci L, Arslan G, Baykara A, *et al.* (2008): Technetium-99m HMPAO brain SPECT in autistic children and their families. Psychiatry Res 162:236–243.
32. Wilcox J, Tsuang MT, Ledger E, Algeo J, Schnurr T (2002): Brain perfusion in autism varies with age. Neuropsychobiology 46:13–16.
33. Gupta SK, Ratnam BV (2009): Cerebral perfusion abnormalities in children with autism and mental retardation: A segmental quantitative SPECT study. Indian Pediatr 46:161–164.
34. Just MA, Keller TA, Malave VL, Kana RK, Varma S (2012): Autism as a neural systems disorder: A theory of frontal-posterior underconnectivity. Neurosci Biobehav Rev 36:1292–1313.
35. Brock J, Brown CC, Boucher J, Rippon G (2002): The temporal binding deficit hypothesis of autism. Dev Psychopathol 14:209–224.
36. Denisova K, Zhao G, Wang Z, Goh S, Huo Y, Peterson BS (2017): Cortical interactions during the resolution of information processing demands in autism spectrum disorders. Brain Behav 7:e00596.
37. Just MA, Cherkassky VL, Keller TA, Minshew NJ (2004): Cortical activation and synchronization during sentence comprehension in high-functioning autism: Evidence of underconnectivity. Brain 127:1811–1821.
38. Belmonte MK, Allen G, Beckel-Mitchener A, Boulanger LM, Carper RA, Webb SJ (2004): Autism and abnormal development of brain connectivity. J Neurosci 24:9228–9231.
39. Ecker C, Ronan L, Feng Y, Daly E, Murphy C, Ginestet CE, *et al.* (2013): Intrinsic gray-matter connectivity of the brain in adults with autism spectrum disorder. Proc Natl Acad Sci U S A 110:13222–13227.
40. Khan S, Gramfort A, Shetty NR, Kitzbichler MG, Ganesan S, Moran JM, *et al.* (2013): Local and long-range functional connectivity is reduced in concert in autism spectrum disorders. Proc Natl Acad Sci U S A 110:3107–3112.
41. Cherkassky VL, Kana RK, Keller TA, Just MA (2006): Functional connectivity in a baseline resting-state network in autism. Neuroreport 17:1687–1690.
42. Monk CS, Peltier SJ, Wiggins JL, Weng SJ, Carrasco M, Risi S, *et al.* (2009): Abnormalities of intrinsic functional connectivity in autism spectrum disorders. Neuroimage 47:764–772.
43. Damarla SR, Keller TA, Kana RK, Cherkassky VL, Williams DL, Minshew NJ, *et al.* (2010): Cortical underconnectivity coupled with preserved visuospatial cognition in autism: Evidence from an fMRI study of an embedded figures task. Autism Res 3:273–279.

44. Dinstein I, Pierce K, Eyler L, Solso S, Malach R, Behrmann M, *et al.* (2011): Disrupted neural synchronization in toddlers with autism. Neuron 70:1218–1225.
45. Lee PS, Yerys BE, Della Rosa A, Foss-Feig J, Barnes KA, James JD, *et al.* (2009): Functional connectivity of the inferior frontal cortex changes with age in children with autism spectrum disorders: A fcMRI study of response inhibition. Cereb Cortex 19:1787–1794.
46. Goh S, Dong Z, Zhang Y, DiMauro S, Peterson BS (2014): Mitochondrial dysfunction as a neurobiological subtype of autism spectrum disorder: Evidence from brain imaging. JAMA Psychiatry 71: 665–671.
47. Madhavarao CN, Chinopoulos C, Chandrasekaran K, Namboodiri MAA (2003): Characterization of the N-acetylaspartate biosynthetic enzyme from rat brain. J Neurochem 86:824–835.
48. Rae CD (2014): A guide to the metabolic pathways and function of metabolites observed in human brain 1H magnetic resonance spectra. Neurochem Res 39:1–36.
49. Clark JB (1998): *N*-acetyl aspartate: A marker for neuronal loss or mitochondrial dysfunction. Dev Neurosci 20:271–276.
50. O'Neill J, Eberling JL, Schuff N, Jagust W, Reed B, Soto G, *et al.* (2000): Method to correlate ^{1}H MRSI and ^{18}FDG-PET. Magn Reson Med 43:244–250.
51. American Psychiatric Association (2000): Diagnostic and Statistical Manual of Mental Disorders, 4th ed, Text Revision. Washington, DC: American Psychiatric Press.
52. Rutter M, Caspi A, Moffitt TE (2003): Using sex differences in psychopathology to study causal mechanisms: Unifying issues and research strategies. J Child Psychol Psychiatry 44:1092–1115.
53. Baron-Cohen S, Wheelwright S, Skinner R, Martin J, Clubley E (2001): The autism-spectrum quotient (AQ): Evidence from Asperger syndrome/high-functioning autism, males and females, scientists and mathematicians. J Autism Dev Disord 31:5–17.
54. Lord C, Risi S, Lambrecht L, Cook EH Jr, Leventhal BL, DiLavore PC, *et al.* (2000): The autism diagnostic observation schedule-generic: A standard measure of social and communication deficits associated with the spectrum of autism. J Autism Dev Disord 30:205–223.
55. Bastiaansen JA, Meffert H, Hein S, Huizinga P, Ketelaars C, Pijnenborg M, *et al.* (2011): Diagnosing autism spectrum disorders in adults: The use of Autism Diagnostic Observation Schedule (ADOS) module 4. J Autism Dev Disord 41:1256–1266.
56. Gotham K, Risi S, Pickles A, Lord C (2007): The Autism Diagnostic Observation Schedule: Revised algorithms for improved diagnostic validity. J Autism Dev Disord 37:613–627.
57. Lord C, Rutter M, Le Couteur A (1994): Autism Diagnostic Interview-Revised: A revised version of a diagnostic interview for caregivers of individuals with possible pervasive developmental disorders. J Autism Dev Disord 24:659–685.
58. Huerta M, Bishop SL, Duncan A, Hus V, Lord C (2012): Application of DSM-5 criteria for autism spectrum disorder to three samples of children with DSM-IV diagnoses of pervasive developmental disorders. Am J Psychiatry 169:1056–1064.
59. Kaufman J, Birmaher B, Brent D, Rao U, Flynn C, Moreci P, *et al.* (1997): Schedule for Affective Disorders and Schizophrenia for School-Age Children-Present and Lifetime Version (K-SADS-PL): Initial reliability and validity data. J Am Acad Child Adolesc Psychiatry 36:980–988.
60. First MB (1997): Structured Clinical Interview for the DSM-IV Axis I Disorders, Patient Edition, version 2.0. New York, NY: Biometrics Research Department, New York State Psychiatric Institute.
61. Wechsler D (1991): Wechsler Intelligence Scale for Children, 3rd ed. San Antonio, TX: Psychological Corporation.
62. Wechsler D (1997): Wechsler Adult Intelligence Scale, 3rd ed. San Antonio, TX: Psychological Corporation.
63. Wechsler D (1999): Wechsler Abbreviated Scale of Intelligence: Manual. San Antonio, TX: Psychological Corporation.
64. Oldfield RC (1971): The assessment and analysis of handedness: The Edinburgh inventory. Neuropsychologia 9:97–113.
65. Hollingshead AB (1975): Four-factor Index of Social Status. New Haven, CT: Yale University Press.
66. Courchesne E (2004): Brain development in autism: Early overgrowth followed by premature arrest of growth. Ment Retard Dev Disabil Res Rev 10:106–111.
67. Herbert MR, Ziegler DA, Makris N, Filipek PA, Kemper TL, Normandin JJ, *et al.* (2004): Localization of white matter volume increase in autism and developmental language disorder. Ann Neurol 55:530–540.
68. Travers BG, Adluru N, Ennis C, Tromp do PM, Destiche D, Doran S, *et al.* (2012): Diffusion tensor imaging in autism spectrum disorder: A review. Autism Res 5:289–313.
69. Ameis SH, Catani M (2015): Altered white matter connectivity as a neural substrate for social impairment in Autism Spectrum Disorder. Cortex 62:158–181.
70. Courchesne E, Pierce K, Schumann CM, Redcay E, Buckwalter JA, Kennedy DP, *et al.* (2007): Mapping early brain development in autism. Neuron 56:399–413.
71. Zikopoulos B, Barbas H (2010): Changes in prefrontal axons may disrupt the network in autism. J Neurosci 30:14595–14609.
72. Harris JJ, Attwell D (2012): The energetics of CNS white matter. J Neurosci 32:356–371.
73. Beirowski B (2013): Concepts for regulation of axon integrity by enwrapping glia. Front Cell Neurosci 7:256.
74. Staugaitis SM, Trapp BD (2009): NG2-positive glia in the human central nervous system. Neuron Glia Biol 5:35–44.
75. Dawson MR, Polito A, Levine JM, Reynolds R (2003): NG2-expressing glial progenitor cells: An abundant and widespread population of cycling cells in the adult rat CNS. Mol Cell Neurosci 24:476–488.
76. Redmond SA, Mei F, Eshed-Eisenbach Y, Osso LA, Leshkowitz D, Shen YA, *et al.* (2016): Somatodendritic expression of JAM2 inhibits oligodendrocyte myelination. Neuron 91:824–836.
77. Fields RD (2015): A new mechanism of nervous system plasticity: Activity-dependent myelination. Nat Rev Neurosci 16:756–767.
78. Yeung MS, Zdunek S, Bergmann O, Bernard S, Salehpour M, Alkass K, *et al.* (2014): Dynamics of oligodendrocyte generation and myelination in the human brain. Cell 159:766–774.
79. Gibson EM, Purger D, Mount CW, Goldstein AK, Lin GL, Wood LS, *et al.* (2014): Neuronal activity promotes oligodendrogenesis and adaptive myelination in the mammalian brain. Science 344:1252304.
80. Young KM, Psachoulia K, Tripathi RB, Dunn SJ, Cossell L, Attwell D, *et al.* (2013): Oligodendrocyte dynamics in the healthy adult CNS: Evidence for myelin remodeling. Neuron 77:873–885.
81. Stevens B, Porta S, Haak LL, Gallo V, Fields RD (2002): Adenosine: A neuron-glial transmitter promoting myelination in the CNS in response to action potentials. Neuron 36:855–868.
82. Orkand RK, Nicholls JG, Kuffler SW (1966): Effect of nerve impulses on the membrane potential of glial cells in the central nervous system of amphibia. J Neurophysiol 29:788–806.
83. Micu I, Plemel JR, Lachance C, Proft J, Jansen AJ, Cummins K, *et al.* (2016): The molecular physiology of the axo-myelinic synapse. Exp Neurol 276:41–50.
84. Almeida RG, Lyons DA (2017): On myelinated axon plasticity and neuronal circuit formation and function. J Neurosci 37:10023–10034.
85. Rivers LE, Young KM, Rizzi M, Jamen F, Psachoulia K, Wade A, *et al.* (2008): PDGFRA/NG2 glia generate myelinating oligodendrocytes and piriform projection neurons in adult mice. Nat Neurosci 11: 1392–1401.
86. Sampaio-Baptista C, Johansen-Berg H (2017): White matter plasticity in the adult brain. Neuron 96:1239–1251.
87. Walhovd KB, Johansen-Berg H, Karadottir RT (2014): Unraveling the secrets of white matter–bridging the gap between cellular, animal and human imaging studies. Neuroscience 276:2–13.
88. Lundgaard I, Osorio MJ, Kress BT, Sanggaard S, Nedergaard M (2014): White matter astrocytes in health and disease. Neuroscience 276:161–173.
89. Haas B, Schipke CG, Peters O, Sohl G, Willecke K, Kettenmann H (2006): Activity-dependent ATP-waves in the mouse neocortex are independent from astrocytic calcium waves. Cereb Cortex 16:237–246.
90. Orthmann-Murphy JL, Freidin M, Fischer E, Scherer SS, Abrams CK (2007): Two distinct heterotypic channels mediate gap junction

coupling between astrocyte and oligodendrocyte connexins. J Neurosci 27:13949–13957.
91. Han X, Chen M, Wang F, Windrem M, Wang S, Shanz S, *et al.* (2013): Forebrain engraftment by human glial progenitor cells enhances synaptic plasticity and learning in adult mice. Cell Stem Cell 12:342–353.
92. Suzuki K, Sugihara G, Ouchi Y, Nakamura K, Futatsubashi M, Takebayashi K, *et al.* (2013): Microglial activation in young adults with autism spectrum disorder. JAMA Psychiatry 70:49–58.
93. Morgan JT, Chana G, Pardo CA, Achim C, Semendeferi K, Buckwalter J, *et al.* (2010): Microglial activation and increased microglial density observed in the dorsolateral prefrontal cortex in autism. Biol Psychiatry 68:368–376.
94. Tetreault NA, Hakeem AY, Jiang S, Williams BA, Allman E, Wold BJ, *et al.* (2012): Microglia in the cerebral cortex in autism. J Autism Dev Disord 42:2569–2584.
95. Masi A, Quintana DS, Glozier N, Lloyd AR, Hickie IB, Guastella AJ (2015): Cytokine aberrations in autism spectrum disorder: A systematic review and meta-analysis. Mol Psychiatry 20:440–446.
96. Rafols JA, Cheng HW, McNeill TH (1989): Golgi study of the mouse striatum: Age-related dendritic changes in different neuronal populations. J Comp Neurol 279:212–227.
97. Lebel C, Walker L, Leemans A, Phillips L, Beaulieu C (2008): Microstructural maturation of the human brain from childhood to adulthood. Neuroimage 40:1044–1055.
98. Terry RD, DeTeresa R, Hansen LA (1987): Neocortical cell counts in normal human adult aging. Ann Neurol 21:530–539.
99. Ando S, Tanaka Y (1990): Synaptic membrane aging in the central nervous system. Gerontology 36(suppl 1):10–14.
100. Grimm A, Eckert A (2017): Brain aging and neurodegeneration: From a mitochondrial point of view. J Neurochem 143:418–431.
101. Werling DM, Geschwind DH (2013): Sex differences in autism spectrum disorders. Current Opinion in Neurology 26:146–153.
102. Halladay AK, Bishop S, Constantino JN, Daniels AM, Koenig K, Palmer K, *et al.* (2015): Sex and gender differences in autism spectrum disorder: Summarizing evidence gaps and identifying emerging areas of priority. Mol Autism 6:36.
103. Haier RJ, Siegel B, Tang C, Abel L, Buchsbaum MS (1992): Intelligence and changes in regional cerebral glucose metabolic rate following learning. Intelligence 16:415–426.
104. Malpas CB, Genc S, Saling MM, Velakoulis D, Desmond PM, O'Brien TJ (2016): MRI correlates of general intelligence in neurotypical adults. J Clin Neurosci 24:128–134.
105. Hallermann S, de Kock CP, Stuart GJ, Kole MH (2012): State and location dependence of action potential metabolic cost in cortical pyramidal neurons. Nat Neurosci 15:1007–1014.
106. Sengupta B, Stemmler M, Laughlin SB, Niven JE (2010): Action potential energy efficiency varies among neuron types in vertebrates and invertebrates. PLoS Comput Biol 6:e1000840.
107. Edgar JM, McCulloch MC, Thomson CE, Griffiths IR (2008): Distribution of mitochondria along small-diameter myelinated central nervous system axons. J Neurosci Res 86:2250–2257.
108. Fruhbeis C, Frohlich D, Kuo WP, Amphornrat J, Thilemann S, Saab AS, *et al.* (2013): Neurotransmitter-triggered transfer of exosomes mediates oligodendrocyte-neuron communication. PLoS Biol 11:e1001604.
109. Kramer-Albers EM, Bretz N, Tenzer S, Winterstein C, Mobius W, Berger H, *et al.* (2007): Oligodendrocytes secrete exosomes containing major myelin and stress-protective proteins: Trophic support for axons? Proteomics Clin Appl 1:1446–1461.
110. Funfschilling U, Supplie LM, Mahad D, Boretius S, Saab AS, Edgar J, *et al.* (2012): Glycolytic oligodendrocytes maintain myelin and long-term axonal integrity. Nature 485:517–521.
111. Saab AS, Tzvetavona ID, Trevisiol A, Baltan S, Dibaj P, Kusch K, *et al.* (2016): Oligodendroglial NMDA Receptors Regulate Glucose Import and Axonal Energy Metabolism. Neuron 91:119–132.
112. Belanger M, Allaman I, Magistretti PJ (2011): Brain energy metabolism: Focus on astrocyte-neuron metabolic cooperation. Cell Metab 14:724–738.
113. Ravera S, Panfoli I, Calzia D, Aluigi MG, Bianchini P, Diaspro A, *et al.* (2009): Evidence for aerobic ATP synthesis in isolated myelin vesicles. Int J Biochem Cell Biol 41:1581–1591.
114. Ravera S, Bartolucci M, Calzia D, Aluigi MG, Ramoino P, Morelli A, *et al.* (2013): Tricarboxylic acid cycle-sustained oxidative phosphorylation in isolated myelin vesicles. Biochimie 95:1991–1998.
115. Morelli A, Ravera S, Panfoli I (2011): Hypothesis of an energetic function for myelin. Cell Biochem Biophys 61:179–187.
116. Harris JJ, Attwell D (2013): Is myelin a mitochondrion? J Cereb Blood Flow Metab 33:33–36.
117. Moffett JR, Ross B, Arun P, Madhavarao CN, Namboodiri AM (2007): N-acetylaspartate in the CNS: From neurodiagnostics to neurobiology. Prog Neurobiol 81:89–131.
118. Francis JS, Strande L, Markov V, Leone P (2012): Aspartoacylase supports oxidative energy metabolism during myelination. J Cereb Blood Flow Metab 32:1725–1736.